1   **Tissue-specific modification of cellular bioelectrical activities using the**

2   **chemogenetic tool, DREADD, in zebrafish**

3

4   Martin R. Silic[1], GuangJun Zhang[1-4*]

5   1. Department of Comparative Pathobiology.

6   2. Purdue University Center for Cancer Research.

7   3. Purdue Institute for Inflammation, Immunology, and Infectious Diseases (PI4D).

8   4. Purdue Institute for Integrative Neuroscience.

9   Purdue University, 625 Harrison Street, West Lafayette, Indiana. 47906. USA.

10

11   * Corresponding author: GuangJun Zhang: Phone: 765-496-1523; Fax: 765-494-9830;

12   Email: gjzhang@purdue.edu

13

14

ABSTRACT

Cellular electronic activity plays an essential role in neuronal communication. Manipulation and visualization of cellular membrane potential remain essential tasks in order to study electrical signaling in living organisms. Light-controlled optogenetic and designed chemical-controlled chemogenetic tools were developed to manipulate cellular electric activities for neuroscience research. One of the most common chemogenetic tools is DREADD (designer receptors exclusively activated by designer drugs). It has been extensively utilized due to its convenience and long-lasting effects in murine and primate models, but not in zebrafish, a leading model organism in various research fields. Here, we first establish multiple tissue-specific transgenic zebrafish lines that express two different DREADDs with a genetically encoded voltage indicator, ASAP2s. We observed voltage changes in zebrafish melanophores, epidermis, and neurons by hM4DGi or rM3DGs receptors measured by ASAP2s fluorescence intensity. Alteration to melanophore bioelectricity by DREADD generated dynamic electric signals and resulted in morphological alterations to pigment cells. We also tested a few agonists and found that the latest generation performs better than clozapine N-oxide (CNO). Collectively, our experiments demonstrate that DREADD can be utilized to manipulate cell-specific membrane potential in the zebrafish model. The availability of this tool in zebrafish will offer a new resource for a variety of bioelectricity research fields such as neuroscience, cardiology, and developmental biology.

37 **KEYWORDS**

38 DREADD, rM3DGs, hM4DGi, DCZ, zebrafish, chemogenetics, GEVI, ASAP2s,

39 bioelectricity, cell voltage manipulation, melanophores

INTRODUCTION

Cellular bioelectric signaling has been extensively investigated in neuromuscular excitable cells due to the important roles of action potential signals and resting membrane potential (1). Recently, accumulating evidence reveals that cellular electric signaling is also an important player for regulating hormone release, embryonic development, wound healing, and regeneration (2,3). Non-invasive perturbation and visualization of cellular electrical activity in real-time and *in vivo* are the central requirements for studying cellular electric signaling (4).

To meet the rapid growth of neuroscience, genetically encoded tools have been developed for perturbation and visualization of cellular bioelectrical activity (5). Channelrhodopsin-based optogenetic tools can enhance or repress neuronal firing on a millisecond scale, and have been successfully applied to elucidate neuron type, activity, circuits, and behaviors (6,7). However, optogenetics generally requires complicated equipment, constrained animals free of movement, and can only modify neuronal activity in the short term (second-minutes). The chemogenetic tools were then developed to meet these needs. Chemogenetics use synthesized small molecules to activate engineered proteins (channels or receptors), modifying cellular electricity over a relatively long period (4,8). DREADDs (Designer receptors exclusively activated by designer drugs) are one group of the most commonly used chemogenetic tools (9,10). The DREADDs are composed of four tools (hM3DGq, rM3DGs, hM4DGi, and KORD) based on different mutated genetically engineered muscarinic receptors. Depending on the downstream G protein-coupled receptor signaling, the DREADD tools can modify cellular bioelectric

62   activity bidirectionally. For example, hM3DGq enhances neuronal excitability, while

63   M4DGi and KORD inhibit cellular excitability. DREADDs have been successfully used to

64   elucidate behavior, circadian disorders, pathways related to cognitive impairments, eating

65   disorders, neuronal plasticity, memory, and more in various animal models (11-14).

66   Furthermore, improvements have been made to increase the selection of ligands with

67   improved specificity and affinity (15-17).

68   Genetically encoded tools for visualizing and measuring cellular electrical activity *in vivo*

69   are equally important for studying cellular electricity. Revolutionary biosensor tools,

70   genetically encoded voltage indicators (GEVIs), for measuring cell membrane voltage

71   have been developed for neuroscience (18-20). These GEVIs measure cellular voltage

72   based on either FRET (fluorescence resonance energy transfer) or levels of fluorescence

73   intensity. The advantages over traditional electrical physiology recording include non-

74   invasive, real-time, and nanosecond sensitivity. Among them, the ASAP1-3 (Accelerated

75   Sensor of Action Potentials) have been applied to a variety of model organisms such as

76   fuit fly, mouse, and zebrafish (21-25).

77   Zebrafish have extensively been used for studying embryonic development and modeling

78   human diseases, including cancer. This is because of the many advantages such as

79   vertebrate biology, tractable genetics, external development,   and early embryo

80   transparency (26,27). We and others demonstrated that ASAP1 reported embryonic

81   cellular voltage changes and neural activities in zebrafish (24,28), and a few optogenetic

82   tools were just successfully adopted to the zebrafish model (29). However, DREADDs

83   have been tested and reported to be non-functional in zebrafish (30). Thus, there is still

84 a critical need for a chemogenetic tool that can modify zebrafish cellular electricity in the

85 long term.

86 Here, we generated DREADD transgenic zebrafish lines and tested their function in

87 zebrafish embryos and larvae using newly developed agonists. We demonstrated that

88 this chemogenetic tool is functional in melanophore, neuron, and epithelial cells. Thus,

89 the DREADD tools and our transgenic zebrafish lines can be an excellent resource for

90 the zebrafish community for investigating cellular electricity.

91

92 **RESULTS**

93 Developing transgenic zebrafish lines to express DREADDs

94 Chemogenetic tools have been demonstrated successfully in neuronal studies with

95 murine and primate models. However, the chemogenetic tools, both DREADD and PSAM

96 (pharmacologically selective effector molecules), were found infective in injected

97 zebrafish embryos (30). Recently, the PSAM tool was reported functional in zebrafish

98 using the Tol2 transposon-based transgenic approach (31). Thus, we reasoned that the

99 DREADD tool might also work in transgenic zebrafish. We then created melanophore-

100 specific transgenic zebrafish lines to co-express hM4DGi and ASAP2s using the *mitfa2.1*

101 promoter (Fig. 1A). This fish will allow us to simultaneously examine bioelectric changes

102 during the process of cell membrane voltage manipulation. Adapting to investigate

103 bioelectricity in multiple tissues, we also take advantage of the Gal4-UAS (Upstream

104 activator sequence) artificial binary gene expression system (Fig.1B) (32). We made

105   zebrafish lines in which a UAS promoter drives either hM4DGi or rM3DGs, together with

106   ASAP2s. Additionally, we made the melanophore (*mitfa2.1* promoter) and basal epithelial

107   cell (*tp63* promoter) specific Gal4FF fish lines (Fig.1C). We chose these two cell types

108   because they are on the surface of the fish embryos, where the agonist chemicals can

109   reach the cells easily, and it is convenient for us to image the cell membrane voltage

110   change. These fish lines allow us to assess the effects of DREADD with different agonists

111   (Fig. 1D). All the transgenic fish were outcrossed with wild type to F_1 or F_2 to clean the

112   genetic background before use for experiments.

113

114   DREADDs work in zebrafish embryos, evidenced by ASAP2s fluorescence intensity

115   changes

116   Since ASAP2s, a sensitive cell membrane voltage reporter, was included in our

117   transgenic zebrafish, we reasoned that the green fluorescence of fish embryos would

118   change if the DREADD tool works. To test this, deschloroclozapine (DCZ), one of the

119   most recently reported highly potent DREADD agonists, was tested with a relatively high

120   dosage by adding 1μL of 100mM DCZ to an imaging slide with about 400μL of fish system

121   water (~250 μM). We treated 2dpf (day post-fertilization) Tg(*mitfa2.1:ASAP2s-IRES-*

122   *hM4DGi*) fish embryos and indeed detected increased fluorescence in the melanophores

123   on the top of the head about 5-10 minutes after treatment (Fig. 2A, D). This increased

124   fluorescence is consistent with the hyperpolarizing activity of hM4DGi. Next, we examined

125   epithelial cells using the fish embryos from Tg(*tp63:Gal4VP16;cryaa:EGFP*) and

126   Tg(*4xnrUAS:ASAP2s-IRES-hM4DGi; cmlc2:EGFP*) fish cross. Similarly, the DCZ

127   treatment resulted in fluorescence intensity increases of the epithelial cells in the head

128   region (Fig. 2B, E) and caudal fin folds (Fig. 2bb, ee). To further test hM4DGi's function

129   in neurons, we first injected the *elavl3* promoter-driven Gal4FF construct into

130   Tg(*4xnrUAS:ASAP2s-IRES-hM4DGi;cmlc2:EGFP*) fish embryos and raised them to 2dpf.

131   Then, we treated the fish embryos with DCZ. As expected, we found the neurons in the

132   neural tube showed enhanced green fluorescence in treated fish embryos (Fig. 2C, F).

133   Thus, the inhibitory DREADD, hM4DGi, is indeed able to induce hyperpolarization within

134   zebrafish. To further test the DREADD tools in zebrafish, we examined the excitable

135   DREADD, rM3DGs. Both melanophores (Fig. 2G, J) and neurons (Fig. 2I, L) showed

136   decreased green fluorescence after DCZ treatment. This decreased green fluorescence

137   is consistent with depolarizing activity of rM3DGs. In contrast, the epithelial cells showed

138   increased green fluorescence (Fig. 2H, K). This unexpected opposite result may be

139   caused by the epithelial cell's physiological response for maintaining its resting

140   membrane potential. Overall, our experiments demonstrated that DCZ could activate both

141   hM4DGi and rM3DGs in zebrafish.

142

143   DREADD activation causes dynamic bioelectric changes in zebrafish melanophores

144   We have demonstrated that DCZ can activate *hM4DGi* in the Tg(*mitfa2.1:ASAP2s-IRES-*

145   *hM4DGi*) fish causing fluorescence to increase after 5-10 minutes. To further examine

146   the exact bioelectric changes that take place after hM4DGi activation leading up to overall

147   fluorescence increase, we decided to record treated larvae with time-lapse imaging

148   immediately. We found that the green fluorescence intensity increase was not linear.

149   Instead, the fluorescence intensity fluctuated, but the overall intensity increased with time

150 extended. In addition, the fluorescence intensity of adjacent melanophores also fluctuated

151 (Fig. 3A-G). These results indicate a melanophore membrane potential homeostasis,

152 which may take time to change using DREADD and its agonist. These results also might

153 indicate why all DREADD expressing cells do not immediately show uniform fluorescence

154 change.

155

156 <u>New generation DREADD agonists are more potent and specific</u>

157 The original DREADD agonist, Clozapine-N-oxide (CNO), was found not as ideal due to

158 its back-conversion to clozapine, an activating molecule with psychoactive properties

159 prescribed to treat schizophrenia. This can have adverse side effects on studies linked to

160 animal behaviors in mouse studies (33). More potent agonists were screened out to

161 overcome this issue. To select the best agonists for DREADDs in zebrafish, we tested

162 Compound 21 (C21) (34), JHU37160 (15), and CNO, then compared them to DCZ . One

163 day old fish embryos were collected from Tg(*mitfa2.1:ASAP2s-IRES-hM4DGi*) fish in-

164 cross and were averaged into four wells in a 6 or 12-well plate. Next, the fish embryos

165 were treated with the four agonists at various concentrations according to previously

166 reported working concentrations for the mammalian system. Twenty-four hours later, the

167 brightest embryos from each well were sorted out and imaged under the same

168 microscope settings and compared to untreated embryos (Fig. 4A-B). Fish embryo

169 images were processed for calculating the corrected total cell fluorescence (CTCF), which

170 is a convenient estimate of fluorescence intensity that takes into account area and

171 background fluorescence. Then, ASAP2s green fluorescence intensities were compared

172 at each concentration of the agonists. For all the agonists, higher concentration resulted

173   in more significant fluorescence changes (Fig. 4C). However, the effective dosage that

174   leads to fluorescence increase varied greatly. CNO and C21 performed the weakest,

175   while the latest generation, JHU37160, and DCZ, had the best response at a dramatically

176   lower dosage. The potency of these agonists in zebrafish is consistent with recent reports

177   in murine systems.

178

179   <u>DREADD functional validation by melanophore morphological changes</u>

180   We successfully modified cell membrane potential that can be measured via the ASAP2s

181   voltage reporter. Whether this DREADD induced voltage change is enough to effect the

182   *in vivo* biology remains unknown. To address this question, we treated

183   Tg(*mitfa2.1:ASAP2s-IRES-hM4DGi*) fish larva with 20uM DCZ at 2dpf then raised them

184   for five days (2dpf-7dpf). We found that the treated fish larvae developed

185   hyperpigmentation compared to the untreated sibling control group (Fig. 5A-B). To figure

186   out whether this melanophore hyperpigmentation was caused by an increased number of

187   melanophores or melanophore dispersion, we treated these fish larva with 1mM

188   epinephrine (α_2-adrenoceptor agonist), which is known to cause melanosome

189   aggregation. Epinephrine caused pigment granule contraction in DCZ treated fish larvae

190   (Fig. 5C-D). Interestingly, embryos treated with epinephrine that were re-treated with DCZ

191   caused pigments to start expanding (Fig 5E). To rule out the possible side effect of DCZ

192   and examine the efficacy of other agonists, we did the same experiment with the other

193   three agonists. The DCZ and JHU37160 agonists have a higher percentage of

194   hyperpigmentated larvae, and a majority of them (81% DCZ and 72.7% JHU37160) are

195   transgenic fish confirmed by post-experimental genotyping of a portion of treated embryos

196   (Table 1). In contrast, the CNO and C21 agonist treatment yielded fewer pigment

197   responses. All the agonist treatments produced a hyperpigmentation phenotype, but DCZ

198   had the lowest off-target rate, suggesting this is a good choice for zebrafish experiments.

199   To test the response of metamorphic melanophores to DREADD induced bioelectric

200   changes, Tg larvae were raised to 2 weeks of development (~6.5mm), and then treated with DCZ

201   (20 µM) for 1 week every 2 days. Fish were then imaged at about 30 days of development (9-

202   10mm) for changes to pigmentation. Comparable-sized untreated transgenic fish were raised as

203   a control. We found that one fish developed an expanded melanophore pigmentation on the

204   lateral sides and fins compared to untreated controls (Fig. 5F-G). In summary, our results

205   confirmed that the DREADD tools indeed are functional and can be used for relevant

206   biological studies.

207

208   **DISCUSSION**

209   The chemogenetic tools are useful for manipulating bioelectricity and have been

210   demonstrated successfully in neuroscience with murine and primate models. DREADD

211   and PSAM tool adaptation was attempted but not successful in zebrafish (30). Recently,

212   we showed that the bioelectricity of the somites is involved in fin patterning (35). To further

213   investigate the roles of bioelectricity during embryonic development, there is a need for

214   chemogenetic tools which allow us to manipulate bioelectricity for days and months. In

215   addition, we have successfully adapted the ASAP1 voltage sensor to zebrafish using the

216   Tol2 transposon-based transgenic approach (24). Recently, the PSAM tools were

217 demonstrated functional in zebrafish using the same transgenic approach (31). This

218 motivated us to re-examine the possibility of adopting DREADDs in zebrafish.

219 There are a few caveat issues that could make a difference between our work and the

220 previous study. First, the sensitivity of the detection method may be a key factor. We use

221 the newly developed ASAP2s, which was reported to have a high level of sensitivity to

222 cellular membrane voltage changes. In comparison, locomotor activity was used for

223 measuring the bioelectric changes previously. It is possible that there is some level of

224 bioelectric change, but not enough to drive the locomotor activity change. Second, we

225 examined the DREADDs using transgenic zebrafish lines, not the direct injection as in the

226 former study. The transgenic fish provide stable and specific DREADD expression in the

227 fish embryos for the targeted tissue. Thus, it reduces many stochastic expressions for

228 measuring electric activities. In contrast, the direct injection of DREADD constructs will

229 yield different levels of expression in many places. Third, we tested a few agonists in our

230 current study and found the formerly used CNO less potent than the newly developed

231 agonists. In our experiments, CNO was able to cause DREADD activation and induce

232 morphological melanophore changes. Still, these results were not as strong and less

233 specific compared to the latest generation DREADD ligands DCZ and JHU37160. The

234 use of CNO could impact the assessment dramatically, especially in the situation of less

235 tissue-specifically expressed DREADDs. When we injected the *elavl3*:Gal4FF plasmid

236 construct into Tg (*UAS*:DREADD-ASAP2s) transgenic fish embryos, only a few larval

237 neurons were observed with fluorescence changes. One solution is to improve the

238 DREADD expression levels. In the future, zebrafish fish-codon optimization, utilizing the

239 zebrafish Kozak sequence before an ATG start codon, and adding dORF (downstream

240   open reading frame) could be attempted for this purpose (36,37). Lastly, the examination

241   time after treatment might also affect the judgment. In our experimental system, a higher

242   concentration of ligands is still needed in order to visualize more impressive fluorescence

243   changes over a shorter period of time (~5minutes). This could be caused by tissue

244   penetration, fish metabolism, or chemical potency.

245   There are numerous zebrafish pigment pattern mutants that affect proteins that regulate

246   charged molecules, such as ion channels and gap junctions (38). Alteration of these ionic

247   regulators can cause morphological changes to zebrafish pigments and disrupt normal

248   stripe formation. It was previously reported that melanophore cell membrane voltage

249   manipulation with the optogenetic tool ChR2 was able to disrupt stripe formation in

250   metamorphic and adult zebrafish (39). Here, we chose zebrafish melanophores as a

251   model and tested two DREADDs, hM4DGi and rM3DGs, and four agonists. We

252   demonstrated that both DREADDs are functional to change cell membrane voltage

253   measured by ASAP2s. These voltage alterations were validated in basal epithelial cells

254   and neurons. Moreover, we were able to generate a melanophore hyperpigmentation

255   phenotype via hM4DGi and DCZ in 1-week larvae, confirming the biological functions of

256   DREADD in zebrafish. hM4DGi activation of metamorphic melanophores also results in

257   hyperpigmentation compared to untreated controls. These results provide additional

258   validation for the biological impact, as well as the potential use of zebrafish DREADDs in

259   older fish over longer periods of time.

260   In summary, we generated tissue-specific DREADD transgenic zebrafish lines and tested

261   their function in zebrafish embryos and larvae using different agonists. We demonstrated

262   that this chemogenetic tool works in zebrafish melanophores, neurons, and epithelial

263   cells. The newly developed agonists are much more potent and specific compared to

264   CNO. We expect the DREADD tools and our transgenic fish lines will meet the critical

265   need for neuronal and embryonic bioelectric studies. Moreover, they can be a great

266   resource to the zebrafish community.

267

268   **MATERIALS AND METHODS**

269   Zebrafish were raised and maintained at the Purdue animal housing facility following

270   Association for Assessment and Accreditation of Laboratory Animal Care (AAALAC)

271   approved standards. Experiments were carried out according to Purdue Animal Care and

272   Use Committee (PACUC) approved protocols. All zebrafish experiments were carried out

273   in wild-type TAB fish. Zebrafish were maintained according to the zebrafish book.

274   Zebrafish embryos were staged based on the Kimmel staging guide.

275

276   **Tol2 constructs, microinjection, and zebrafish transgenic lines**

277   Tol2 transposon plasmids were generated using three-fragment Gateway cloning-based

278   Tol2 kit (40).The 5' end entry plasmids p5E-*mitfa2.1 (plasmid #81234)*, p5E-*elavl3*

279   (plasmid #72640) (41), p5E-4xrnUAS (plasmid #61372) (42) were acquired through

280   Addgene. pME-Gal4FF were subcloned from pCR8GW-Gal4-VP16-FRT-kan-FRT (43), a

281   gift from Dr. Koichi Kawakami. p5E-tp63 was a gift from Dr. Qing Deng (44). The pENTR-

282   D-ASAP2s plasmids were generated by site-directed mutagenesis from pENTR-D-

283   ASAP1 (24) using the primers (ASAP2s-F: ATA TTT CAG CTG GCT TCA CAG AAG

284   AAA CAA CTT GAA GTG G and ASAP2s-R: AGC CAG CTG AAA TAT TCT TAT TAA

285   GAT AAC AAT TCT CAG AAC TCG AAG AAG AG). The p3E-*IRES-hM4DGi* and p3E-

286   *IRES-rM3DGs* were generated by subcloning from pAAV-hSyn-DIO-HA-hM4DGi-IRES-

287   mCitrine (plasmid# 50455) and pAAV-hSyn-DIO-HA-rM3DGs-IRES-mCitrine (pasmid#

288   50456) into p3E-IRES-EGFP vector (Tol2 kit #389), respectively. All the subcloning and

289   site-directed mutagenesis were performed using the In-Fusion cloning system (Takara

290   Bio). Final entry constructs were verified by Sanger sequencing. The final constructs were

291   built using LR Clonase II Plus enzyme (Thermo Scientific) following the manufacturer's

292   instructions.

293

294   pCS-zT2Tp plasmid (a gift from Koichi Kawakami) was used as a template to generate

295   Tol2 transposase messenger RNA (mRNA) using the mMESSAGE mMACHINE SP6

296   transcription kit (Thermo Scientific). Capped and tailed mRNAs were purified by Monarch

297   RNA Cleanup Kit (NEB) according to the manufactory guide and eluted in DEPC-treated

298   water. Microinjection of Tol2 expression constructs (25 ng/µl) and Tol2 mRNA (50 ng/µl)

299   with 0.025% phenol red (P0290; Sigma) was performed on one-cell-stage zebrafish

300   embryos under a dissection microscope (SMZ445; Nikon, Garden City, NY) using a

301   PV820 pneumatic PicoPump (World Precision Instruments). About ten injected embryos

302   were sampled for gDNA isolation using the HotSHOT method after at least 8 hours (45).

303   Tol2 transposon efficiency was verified with an excise assay (46). Once the excise assays

304   confirmed the Tol2 activity, the remainder of the injected fish embryos were raised to

305   adulthood. TAB wild-type fish were crossed with F_0-injected adult fish, and positive

306   fluorescent transgenic zebrafish embryos were selected and raised to adults as stable

307   F_1 transgenic fish lines.

308

DREADD ligand addition and fluorescence imaging

310   To detect cell membrane potential changes via ASAP2s imaging, embryos were raised

311   to 2 days post fertilization (dpf), then anesthetized in a 0.05% Tricane solution. For

312   fluorescence imaging experiments, embryos were raised in fish system water without

313   methylene blue to reduce autofluorescence and treated with 1X PTU (1-phenyl 2-

314   thiourea, 0.2mM) to reduce pigments. Anesthetized embryos were placed on a glass slide

315   with fish system water and positioned properly for imaging. In order to visualize large

316   changes in fluorescence intensity, 1μL of 100mM DCZ was added to slides containing Tg

317   fish and ~400μL of fish water for a final concentration of 250 μM. Untreated images were

318   taken before agonist addition. After treatment, embryos were either monitored for 5-15

319   minutes for fluorescence changes and then imaged, or immediately recorded with time-

320   lapse imaging. Exposure was set at the start of imaging (between 4000 and 8000 ms)

321   and kept consistent for the entire length of time the same individual larva was imaged in

322   order to compare levels of fluorescence intensity between images directly. All the

323   DREADD agonists were purchased from HelloBio and diluted in water as 100mM stock

324   solutions that were stored in a -20C freezer before use. Described concentrations of

325   DREADD agonist were then added to the fish system water on the slide. Embryos were

326   monitored for positional shifts and adjusted if they drifted from their original location. Next,

327   time-lapse imaging was continued for 5-15 minutes. Cellular $\Delta F/F=((F_t - F_0)/F_0)$ was

328   quantified using ImageJ to define a region of interest for mean fluorescence intensity at

329   each time point. F_t is the fluorescent value at a given time t, and F_0 is the starting

330   fluorescence value. All images were acquired using Zeiss Axio CamMRc camera on

331   Stereo Discovery.V12 or Axio Imager 2 compound microscope. For *elavl3*:Gal4FF, Tol2

332   plasmid was injected into 1-cell stage Tg (*UAS*:DREADD-ASAP2s) transgenic fish

333   embryos. UAS fish lines were prepared for one-cell-stage microinjection as described

334   above. Injected embryos were monitored and raised to 2dpf. Embryos with positive

335   fluorescence, via GFP eye and heart markers, were sorted and used for agonist addition

336   and fluorescence imaging, as previously mentioned. Unless specified otherwise, this type

337   of signal is expressed as a fractional change in fluorescence intensity ΔF/F0.

338

339   **Quantifying fluorescence intensity from different ligand concentrations**

340   About 25 Tg (*mitfa2.1*: *ASAP2s-IRES-hM4DGi*) embryos were treated with designated

341   concentrations of ligands at 1dpf in 12-well plates. The following day, two embryos with

342   the brightest fluorescence in each well were imaged with the same exposure and

343   magnification. Images were later processed for corrected total cell fluorescence (CTCF)

344   by subtracting the mean background intensity multiplied by the area for the ROI from

345   the integrated density of fish head fluorescence (integrated density - (ROI area* mean

346   background intensity). Values were then normalized to 1 for the untreated samples.

347

348   **Tracking 1-week larvae for DREADD induced phenotype**

349 To track pigmentation changes caused by DREADD treatments, we crossed Tg

350 (*mitfa2.1*: *ASAP2s-IRES-hM4DGi*) with TAB fish. Dechorionated 2dpf embryos were

351 separated into groups of about 40 and placed into 6-well plates containing fish water

352 with 0.05% methylene blue. This mixed group of siblings contained wildtype and

353 transgenic larvae. Next, the water was replaced with fresh water containing a

354 designated concentration of DREADD agonists. Embryos were treated once at 2dpf and

355 raised until 7dpf. At 7dpf, larvae in each well were counted to obtain the number with

356 increased head pigmentation. This was repeated, and both trials later added to the total

357 number of fish tracked for each DREADD agonist (n=128).

358 For genotyping a representative portion of DREADD treated embryos, 96-well plates

359 were used to separate single embryos from Tg (*mitfa2.1*: *ASAP2s-IRES-hM4DGi*)

360 crossed with wildtype fish. Dechorionated 2dpf embryos were separated and placed into

361 individual wells containing fish water with methylene blue. This mixed group of siblings

362 contained wildtype and transgenic larvae. Next, water was replaced with 200uL of fresh

363 fish water containing designated amounts of DREADD ligand. These two-day-old fish

364 embryos were treated with either DCZ, JHU37160, C21, or CNO (n=48 for each

365 agonist), respectively. Each well was tracked until seven days to observe pigmentation

366 changes. On the 7th day, the number of embryos with increased head pigmentation was

367 counted. All embryos were then harvested for genotype using 100mM NaOH (hotshot

368 method). PCR primers (ASAP1-genoF: ATA TGA CCT ACT CCT TCT CTG ACC and

369 ASAP1-genoR: AGG TTA AGG TGG TCA CCA GG) were used to amplify the ASAP2s

370 transgene to validate transgenic mutant correlation with phenotypic changes. These

371   percentages were caculated as a representative of a total of 128 tracked embryos for

372   each agonist.

373   For examining the variation of melanophore morphology, 7dpf Larvae were treated with

374   epinephrine (1mM) to determine any changes to total pigment count and assess

375   pigment expansion. Larvae were placed on a glass slide with fish system water and

376   imaged under regular epifluorescent light. For evaluating the impact of bioelectric

377   changes on metamorphic fish melanophores, transgenic larvae that were about two

378   weeks of development (~6.5mm) were treated with DCZ (20 μM) for one week every

379   two days. Once fish reached about 30 days old (9-10mm), they were imaged under a

380   microscope for pigmentation changes. Comparable-sized untreated transgenic fish were

381   also imaged as a control.

382

388

389   **AUTHOR CONTRIBUTIONS**

390   G.Z. conceptualization; M.R.S. and G.Z. formal analysis; G.Z. funding acquisition; M.R.S.

391   and G.Z. Investigation; G.Z. Supervision; M.R.S. and G.Z. writing, review, and editing.

392

393   **COMPETING INTERESTS**

394   The authors declare no competing interests.

395

396

397 **Fig.1. Illustration of DREADD transgenic fish lines and experimental workflow. A.**

398 Tol2 construct and method to produce stable DREADD zebrafish line, Tg (*mitfa2.1:*

399 *ASAP2s-IRES-hM4DGi*). X, fish cross. Black arrow, fish raising or produced. **B.**

400 Illustration of principles of the Gal4-UAS system. **C.** Diagrams of the Tol2 transposon

401 plasmid constructs used for the Gal4-UAS transgenic zebrafish lines. The Gal4 fish lines

402 have an eye maker (green), *cryaa:EGFP*. The UAS fish lines have a heart marker (green),

403 *cmlc2:EGFP*. X, fish cross. Black arrow, fish raising or produced. Tol2, Tol2 transposon

404 minimal flanking DNA sequences. IRES, internal ribosome entry site. **D.** Basic workflow:

405 DREADD agonists were used to treating transgenic DREADD zebrafish embryos to cause

406 cell bioelectric changes, then the fish embryos were subjected to green fluorescence

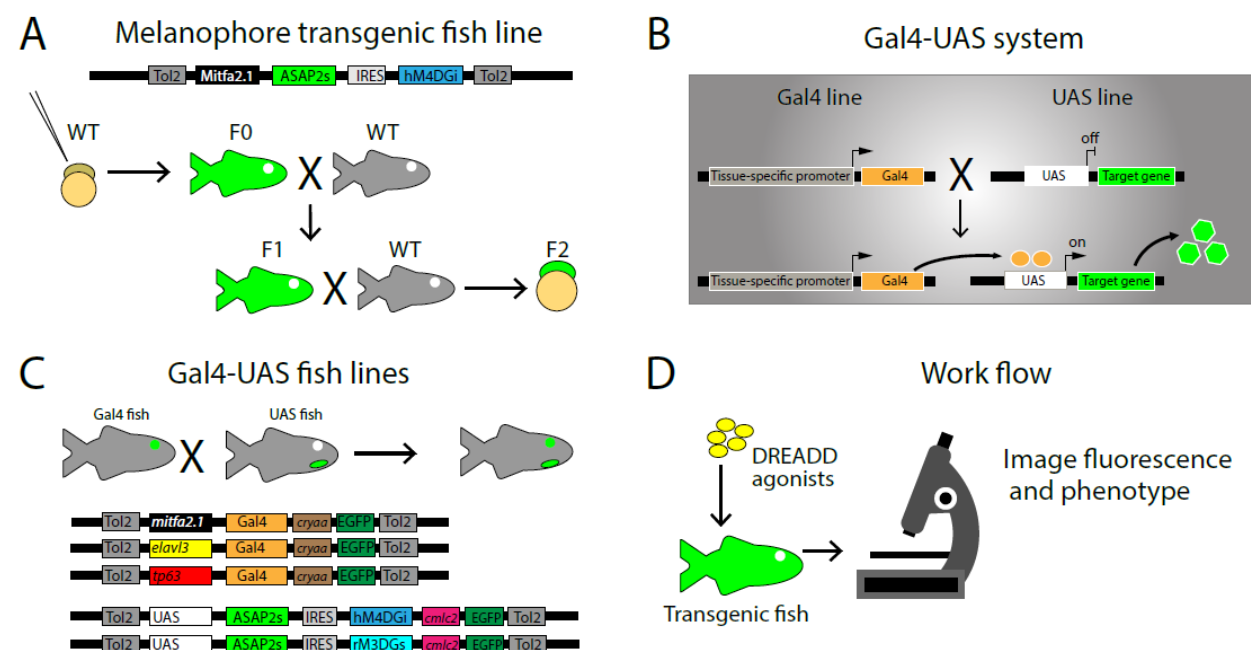407 imaging and quantification.

408

409

Fig. 2. Cell membrane voltage manipulation by DREADD in zebrafish embryos. A-F. Transgenic zebrafish expressing ASAP2s-IRES-hM4DGi in melanophore (*mitfa2.1*), basal epithelial cell (*tp63*), or neuron (*elavl3*) promoter, respectively. **A-C**. Fish embryos before DCZ treatment. **D-F**. The same fish corresponding to the **A-C** panels after treatment with DCZ. Inserts **bb** & **ee:** caudal fin images of Tg(*tp63:ASAP2s-IRES-hM4DGi*) fish before and after DCZ treatment, respectively. Yellow arrows indicate specific cells with increased levels of fluorescence. **G-L.** Transgenic zebrafish expressing ASAP2s-IRES-hM3DGs in melanophore (*mitfa2.1*), basal epithelial cell (*tp63*), or neuron (*elavl3*) promoter, respectively. **G-I**. Fish embryos before DCZ treatment. **J-L.** The same fish corresponding to the **G-I** panels after treatment of DCZ. Panels (**A**, **D**) with red dotted lines are from a cross between the Tg(*mitfa2.1*:ASAP2s-*IRES-hM4DGi*) and wild type. Panels (**C**, **F**, **I**, **L**) with blue dotted lines were from Tg(*UAS:ASAP2s-IRES-hM4DGi*) or Tg(*UAS:ASAP2s-IRES-hM3DGs*) fish injected with *elavl3*:Gal4FF plasmid construct. The remaining panels (**B**, **E**, **G-H**, **J-K**) were offspring from crosses of Gal4 and UAS transgenic fish lines. All the fish embryos are two days old. Yellow arrows indicate specific cells with altered levels of fluorescence. Only matching (before and after DCZ treated) embryos are directly comparable for fluorescence intensity levels (**A** & **D**, **B** & **E**, **C** & **F**, **G** & **J**, **H** & **K**, **I** & **L**.) Scale bars = 250 µm except for panel inserts **bb** and **ee** where scale bar = 50 µm.

429

430

431
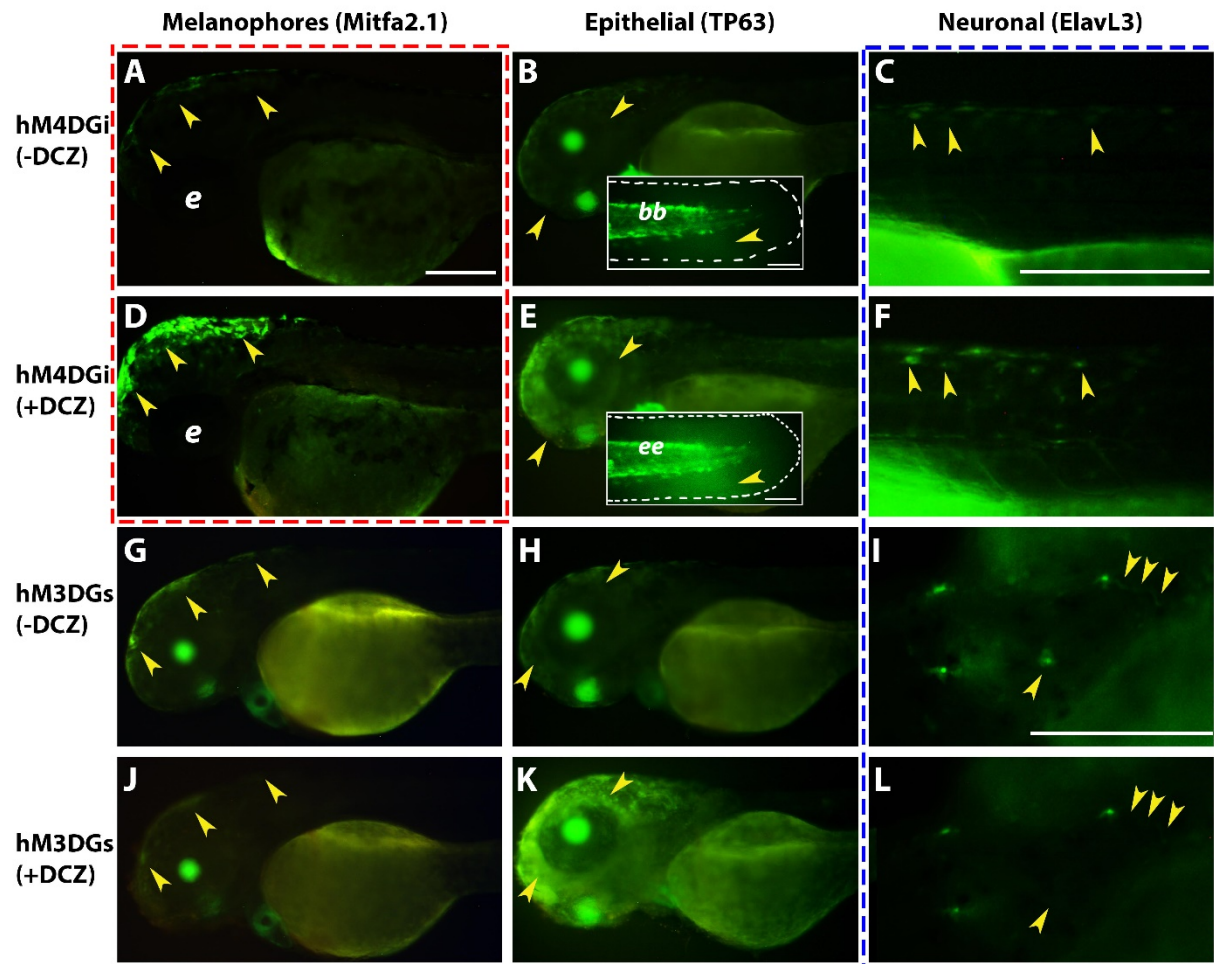
Fig. 3. Melanophores show dynamic fluorescence changes after DREADD modification. A-F. Six different time points of melanophore imaging in the head region of a 2dpf Tg(*mitfa2.1*:ASAP2s-*IRES-hM4DGi*) zebrafish embryo after DREADD activation. The time scale is in seconds. Arrows point to changes in GFP intensity in the same location. **G.** ΔF/F quantification of melanophore fluorescence intensity changes

437   over a 6-minute duration. ASAP2s fluorescence shows fluctuations in intensity. Scale bar

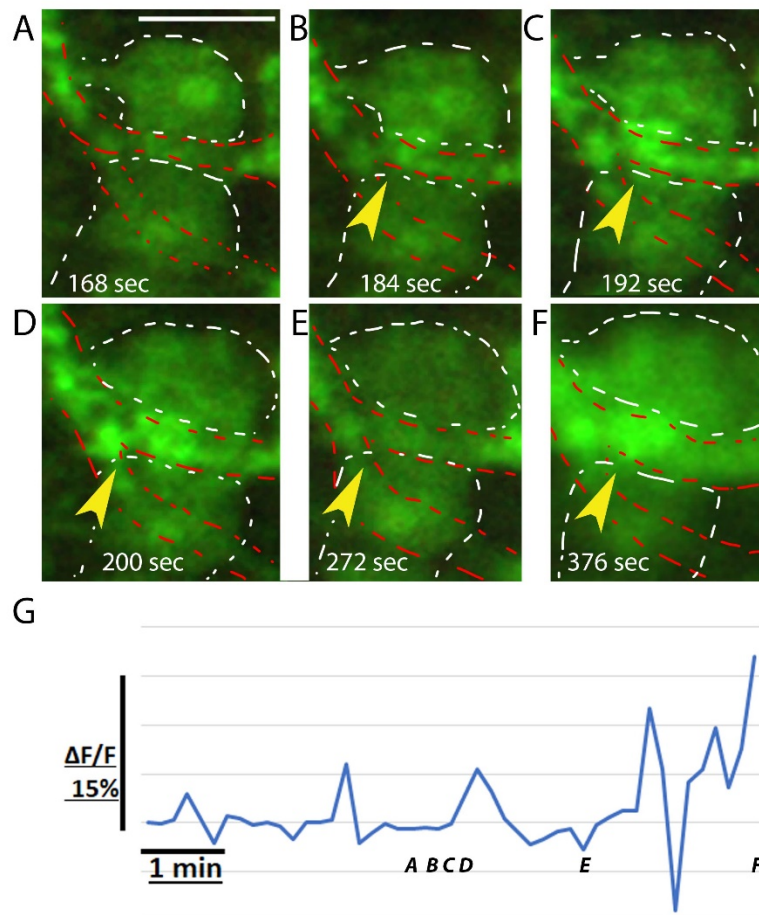438   = 25 µm. The corresponding time-lapse video can be found in the Supplementary file S1.

439

440

441   **Fig. 4. New DREADD agonists, DCZ, and JHU37160 have higher efficacy. A.** A

442   representative embryo from the Tg(*mitfa2.1*:ASAP2s-*IRES-hM4DGi*) zebrafish. The

443   melanophores in the head region display minimal green fluorescence. **B.** A representative

444   embryo shows bright pigment fluorescence after agonist treatment. **C.** Quantification of

445   corrected total cell fluorescence (CTCF) after 24-hour treatment with different

446   concentrations of CNO, C21, JHU37160, and DCZ. The concentrations (μM) are labeled

447   in the vertical bars with different colors. All the fish embryos are two days old. Scale bars

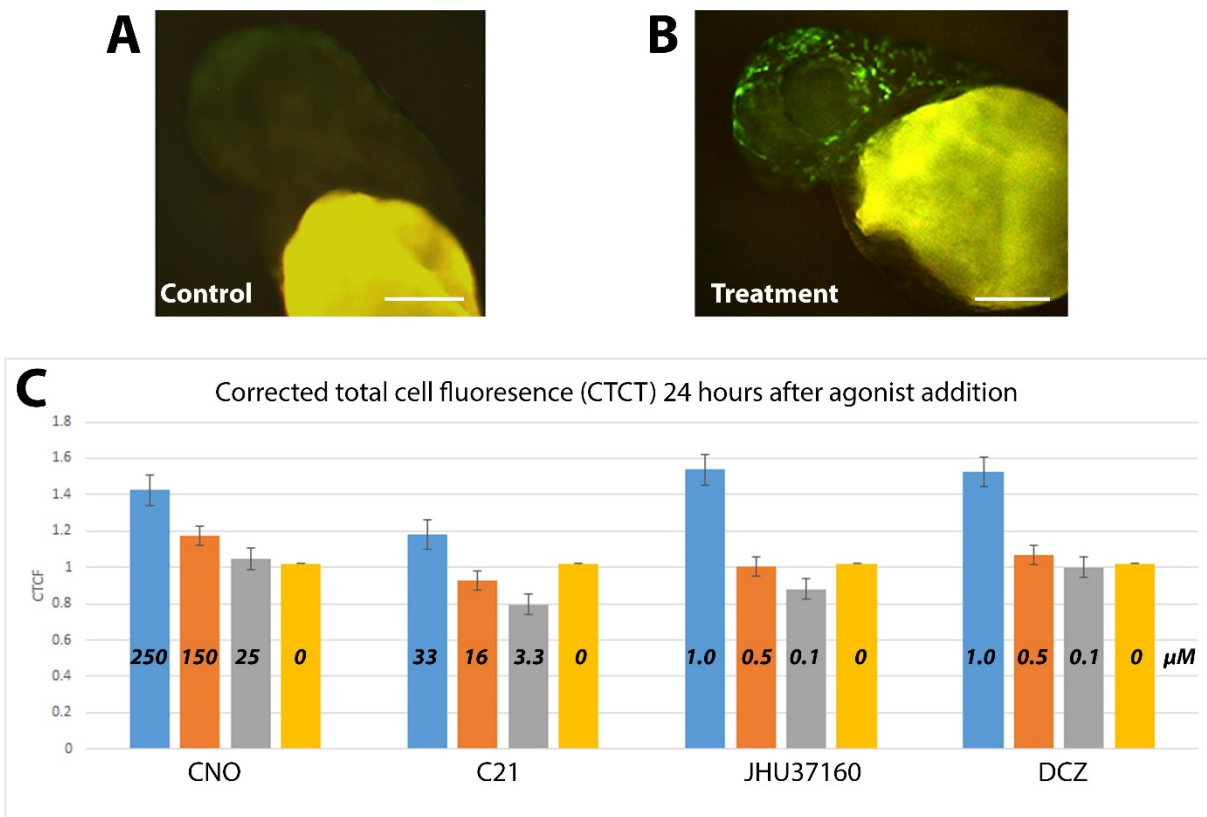448   = 250 μm.

449

450

Fig. 5. The hM4DGi receptor activation causes hyperpigmentation in 1-week old

and metamorphic fish larvae. **A.** A representative untreated 1-week old fish larva. **B.** A

representative treated fish larva with hyperpigmentation (circled with red dotted line). **C.**

Dorsal view of another Tg(*mitfa2.1*:ASAP2s-*IRES-hM4DGi*) fish larva that was treated

with DCZ. The melanophores are dispersed. **D.** The same fish larva imaged 3 minutes

after treatment with 1mM epinephrine. The melanophores are aggregated. **E.** The same

457   epinephrine-treated larva was re-treated with DCZ. The image was taken 8 minutes after

458   treatment. The melanophores dispersed again. Yellow arrows point to melanophores that

459   are dispersed, contracted, and re-dispersed, respectively. **F.** 9.4mm fish that was treated

460   with DCZ for one week (20 µM) every two days starting at about 6.5mm of development.

461   Melanophores appear to be dispersed over a larger area. **G.** Comparable sized untreated

462   transgenic fish. Melanophores appear smaller and more uniform. Scale bar = 250 µm for
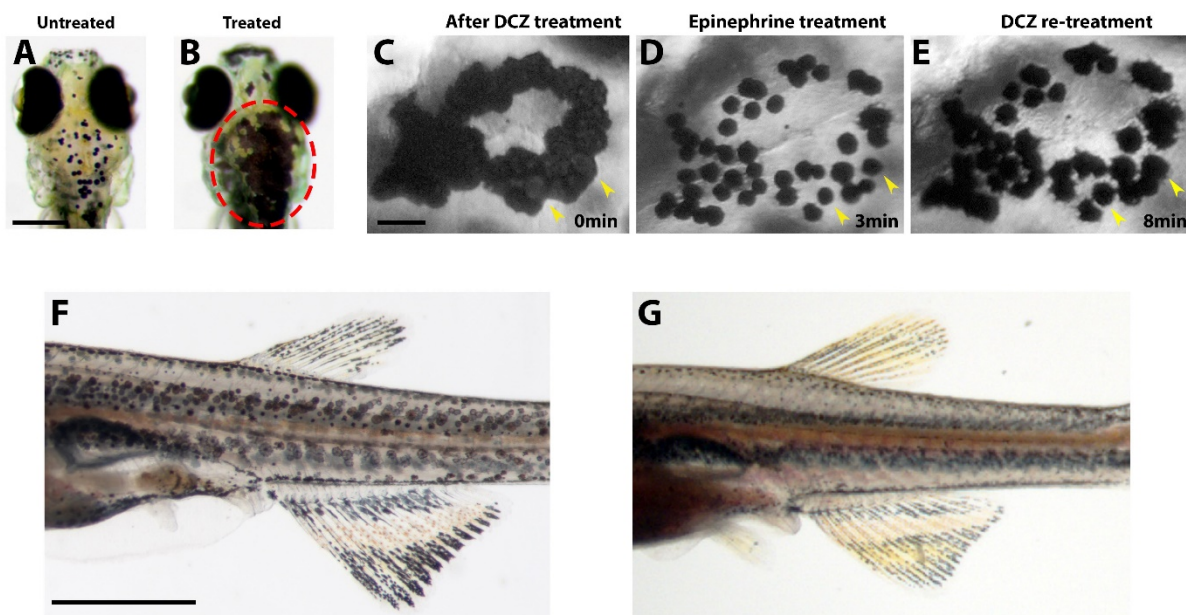
463   **A-B** and 50 µm for **C-E**.

464

465

466

467   **Table 1. Zebrafish larva pigmentation change is caused by different DREADD**

468   **agonists.**

Larval genetic background	DCZ	JHU37160	CNO	C21
Mixed transgenic and wildtype siblings with pigmentation change	49.20%	60.10%	39.00%	8.60%
Genotype confirmed positive transgenic embryos with pigment change	81.00%	72.70%	60%	50%
Wildtype embryos treated with pigmentation change	5.50%	17.90%	12.50%	5%
Untreated transgenic embryos with pigmentation change	1.25%	3.75%	2.50%	1.25%

469

470

REFERENCES

1.   Purves, D., Augestine, G. J., Firzpatrick, D., Hall, W. C., LaMantia, A. S., McNamara, J. O., and Williams, S. M. (2004) *Neuroscience*, 3rd ed., Sinauer Associates, Inc, Sunderland, Massachusetts U.S.A

2.   Harris, M. P. (2021) Bioelectric signaling as a unique regulator of development and regeneration. *Development* **148**

3.   Levin, M. (2021) Bioelectric signaling: Reprogrammable circuits underlying embryogenesis, regeneration, and cancer. *Cell* **184**, 1971-1989

4.   Sternson, S. M., and Roth, B. L. (2014) Chemogenetic tools to interrogate brain functions. *Annu. Rev. Neurosci.* **37**, 387-407

5.   Luo, L., Callaway, E. M., and Svoboda, K. (2018) Genetic Dissection of Neural Circuits: A Decade of Progress. *Neuron* **98**, 865

6.   Grosenick, L., Marshel, J. H., and Deisseroth, K. (2015) Closed-loop and activity-guided optogenetic control. *Neuron* **86**, 106-139

7.   Fenno, L., Yizhar, O., and Deisseroth, K. (2011) The development and application of optogenetics. *Annu. Rev. Neurosci.* **34**, 389-412

8.   Atasoy, D., and Sternson, S. M. (2018) Chemogenetic Tools for Causal Cellular and Neuronal Biology. *Physiol. Rev.* **98**, 391-418

9.   Roth, B. L. (2016) DREADDs for Neuroscientists. *Neuron* **89**, 683-694

10.   Urban, D. J., and Roth, B. L. (2015) DREADDs (designer receptors exclusively activated by designer drugs): chemogenetic tools with therapeutic utility. *Annu. Rev. Pharmacol. Toxicol.* **55**, 399-417

11.   Bonaventura, J., Eldridge, M. A. G., Hu, F., Gomez, J. L., Sanchez-Soto, M., Abramyan, A. M., Lam, S., Boehm, M. A., Ruiz, C., Farrell, M. R., Moreno, A., Galal Faress, I. M., Andersen, N., Lin, J. Y., Moaddel, R., Morris, P. J., Shi, L., Sibley, D. R., Mahler, S. V., Nabavi, S., Pomper, M. G., Bonci, A., Horti, A. G., Richmond, B. J., and Michaelides, M. (2019) High-potency ligands for DREADD imaging and activation in rodents and monkeys. *Nature communications* **10**, 4627

12.   Carter, M. E., Soden, M. E., Zweifel, L. S., and Palmiter, R. D. (2013) Genetic identification of a neural circuit that suppresses appetite. *Nature* **503**, 111-+

13.   Vardy, E., Robinson, J. E., Li, C., Olsen, R. H. J., DiBerto, J. F., Giguere, P. M., Sassano, F. M., Huang, X. P., Zhu, H., Urban, D. J., White, K. L., Rittiner, J. E., Crowley, N. A., Pleil, K. E., Mazzone, C. M., Mosier, P. D., Song, J., Kash, T. L., Malanga, C. J., Krashes, M. J., and Roth, B. L. (2015) A New DREADD Facilitates the Multiplexed Chemogenetic Interrogation of Behavior. *Neuron* **86**, 936-946

14.   Ferguson, S. M., Phillips, P. E. M., Roth, B. L., Wess, J., and Neumaier, J. F. (2013) Direct-Pathway Striatal Neurons Regulate the Retention of Decision-Making Strategies. *J. Neurosci.* **33**, 11668-11676

15.   Bonaventura, J., Eldridge, M. A. G., Hu, F., Gomez, J. L., Sanchez-Soto, M., Abramyan, A. M., Lam, S., Boehm, M. A., Ruiz, C., Farrell, M. R., Moreno, A., Faress, I. M. G., Andersen, N., Lin, J. Y., Moaddel, R., Morris, P. J., Shi, L., Sibley, D. R., Mahler, S. V., Nabavi, S., Pomper, M. G., Bonci, A., Horti, A. G., Richmond, B. J., and Michaelides, M. (2019) High-potency ligands for DREADD imaging and activation in rodents and monkeys. *Nat Commun* **10**

515   16.   Nagai, Y., Miyakawa, N., Takuwa, H., Hori, Y., Oyama, K., Ji, B., Takahashi, M.,
516   Huang, X. P., Slocum, S. T., DiBerto, J. F., Xiong, Y., Urushihata, T., Hirabayashi, T.,
517   Fujimoto, A., Mimura, K., English, J. G., Liu, J., Inoue, K., Kumata, K., Seki, C., Ono,
518   M., Shimojo, M., Zhang, M. R., Tomita, Y., Nakahara, J., Suhara, T., Takada, M.,
519   Higuchi, M., Jin, J., Roth, B. L., and Minamimoto, T. (2020) Deschloroclozapine, a
520   potent and selective chemogenetic actuator enables rapid neuronal and behavioral
521   modulations in mice and monkeys. *Nat. Neurosci.* **23**, 1157-+
522   17.   Chen, X., Choo, H., Huang, X. P., Yang, X. B., Stone, O., Roth, B. L., and Jin, J. (2015)
523   The First Structure-Activity Relationship Studies for Designer Receptors Exclusively
524   Activated by Designer Drugs. *ACS Chem. Neurosci.* **6**, 476-484
525   18.   Bando, Y., Grimm, C., Cornejo, V. H., and Yuste, R. (2019) Genetic voltage indicators.
526   *BMC Biol.* **17**
527   19.   Yang, H. H., and St-Pierre, F. (2016) Genetically Encoded Voltage Indicators:
528   Opportunities and Challenges. *J. Neurosci.* **36**, 9977-9989
529   20.   Lee, S., Song, Y. K., and Baker, B. J. (2019) Engineering Photoactivatability in
530   Genetically Encoded Voltage and pH Indicators. *Front. Cell. Neurosci.* **13**
531   21.   Chamberland, S., Yang, H. H., Pan, M. M., Evans, S. W., Guan, S., Chavarha, M., Yang,
532   Y., Salesse, C., Wu, H., Wu, J. C., Clandinin, T. R., Toth, K., Lin, M. Z., and St-Pierre,
533   F. (2017) Fast two-photon imaging of subcellular voltage dynamics in neuronal tissue
534   with genetically encoded indicators. *eLife* **6**
535   22.   St-Pierre, F., Marshall, J. D., Yang, Y., Gong, Y., Schnitzer, M. J., and Lin, M. Z. (2014)
536   High-fidelity optical reporting of neuronal electrical activity with an ultrafast fluorescent
537   voltage sensor. *Nat. Neurosci.* **17**, 884-889
538   23.   Villette, V., Chavarha, M., Dimov, I. K., Bradley, J., Pradhan, L., Mathieu, B., Evans, S.
539   W., Chamberland, S., Shi, D. Q., Yang, R. Z., Kim, B. B., Ayon, A., Jalil, A., St-Pierre,
540   F., Schnitzer, M. J., Bi, G. Q., Toth, K., Ding, J., Dieudonne, S., and Lin, M. Z. (2019)
541   Ultrafast Two-Photon Imaging of a High-Gain Voltage Indicator in Awake Behaving
542   Mice. *Cell* **179**, 1590-+
543   24.   Silic, M. R., and Zhang, G. (2018) Visualization of Cellular Electrical Activity in
544   Zebrafish Early Embryos and Tumors. *J Vis Exp*, e57330
545   25.   Bando, Y., Sakamoto, M., Kim, S., Ayzenshtat, I., and Yuste, R. (2019) Comparative
546   Evaluation of Genetically Encoded Voltage Indicators. *Cell reports* **26**, 802-+
547   26.   Lieschke, G. J., and Currie, P. D. (2007) Animal models of human disease: zebrafish
548   swim into view. *Nat Rev Genet* **8**, 353-367
549   27.   Santoriello, C., and Zon, L. I. (2012) Hooked! Modeling human disease in zebrafish. *J.*
550   *Clin. Invest.* **122**, 2337-2343
551   28.   Miyazawa, H., Okumura, K., Hiyoshi, K., Maruyama, K., Kakinuma, H., Amo, R.,
552   Okamoto, H., Yamasu, K., and Tsuda, S. (2018) Optical interrogation of neuronal
553   circuitry in zebrafish using genetically encoded voltage indicators. *Sci. Rep.* **8**
554   29.   Antinucci, P., Dumitrescu, A., Deleuze, C., Morley, H. J., Leung, K., Hagley, T., Kubo,
555   F., Baier, H., Bianco, I. H., and Wyart, C. (2020) A calibrated optogenetic toolbox of
556   stable zebrafish opsin lines. *eLife* **9**
557   30.   Chen, S. J., Chiu, C. N., McArthur, K. L., Fetcho, J. R., and Prober, D. A. (2016) TRP
558   channel mediated neuronal activation and ablation in freely behaving zebrafish. *Nature*
559   *Methods* **13**, 147-+

560 31. Beckwith-Cohen, B., Holzhausen, L. C., Nawy, S., and Kramer, R. H. (2020) Controlling
561   Horizontal Cell-Mediated Lateral Inhibition in Transgenic Zebrafish Retina with
562   Chemogenetic Tools. *eNeuro* **7**
563 32. Scheer, N., and Campos-Ortega, J. A. (1999) Use of the Gal4-UAS technique for targeted
564   gene expression in the zebrafish. *Mech. Dev.* **80**, 153-158
565 33. Gomez, J. L., Bonaventura, J., Lesniak, W., Mathews, W. B., Sysa-Shah, P., Rodriguez,
566   L. A., Ellis, R. J., Richie, C. T., Harvey, B. K., Dannals, R. F., Pomper, M. G., Bonci, A.,
567   and Michaelides, M. (2017) Chemogenetics revealed: DREADD occupancy and
568   activation via converted clozapine. *Science* **357**, 503-507
569 34. Chen, X., Choo, H., Huang, X. P., Yang, X., Stone, O., Roth, B. L., and Jin, J. (2015) The
570   first structure-activity relationship studies for designer receptors exclusively activated by
571   designer drugs. *ACS Chem. Neurosci.* **6**, 476-484
572 35. Silic, M. R., Wu, Q., Kim, B. H., Golling, G., Chen, K. H., Freitas, R., Chubykin, A. A.,
573   Mittal, S. K., and Zhang, G. (2020) Potassium Channel-Associated Bioelectricity of the
574   Dermomyotome Determines Fin Patterning in Zebrafish. *Genetics*
575 36. Wu, Q., Wright, M., Gogol, M. M., Bradford, W. D., Zhang, N., and Bazzini, A. A.
576   (2020) Translation of small downstream ORFs enhances translation of canonical main
577   open reading frames. *EMBO J.* **39**, e104763
578 37. Horstick, E. J., Jordan, D. C., Bergeron, S. A., Tabor, K. M., Serpe, M., Feldman, B., and
579   Burgess, H. A. (2015) Increased functional protein expression using nucleotide sequence
580   features enriched in highly expressed genes in zebrafish. *Nucleic Acids Res.* **43**
581 38. Singh, A. P., and Nusslein-Volhard, C. (2015) Zebrafish Stripes as a Model for
582   Vertebrate Colour Pattern Formation. *Curr. Biol.* **25**, R81-R92
583 39. Aramaki, T., and Kondo, S. (2020) Method for disarranging the pigment pattern of
584   zebrafish by optogenetics. *Dev. Biol.* **460**, 12-19
585 40. Kwan, K. M., Fujimoto, E., Grabher, C., Mangum, B. D., Hardy, M. E., Campbell, D. S.,
586   Parant, J. M., Yost, H. J., Kanki, J. P., and Chien, C. B. (2007) The Tol2kit: a multisite
587   gateway-based construction kit for Tol2 transposon transgenesis constructs. *Dev. Dyn.*
588   **236**, 3088-3099
589 41. Fowler, D. K., Stewart, S., Seredick, S., Eisen, J. S., Stankunas, K., and Washbourne, P.
590   (2016) A MultiSite Gateway Toolkit for Rapid Cloning of Vertebrate Expression
591   Constructs with Diverse Research Applications. *PLoS One* **11**, e0159277
592 42. Akitake, C. M., Macurak, M., Halpern, M. E., and Goll, M. G. (2011) Transgenerational
593   analysis of transcriptional silencing in zebrafish. *Dev. Biol.* **352**, 191-201
594 43. Suster, M. L., Abe, G., Schouw, A., and Kawakami, K. (2011) Transposon-mediated
595   BAC transgenesis in zebrafish. *Nat. Protoc.* **6**, 1998-2021
596 44. Zhou, W., Pal, A. S., Hsu, A. Y., Gurol, T., Zhu, X., Wirbisky-Hershberger, S. E.,
597   Freeman, J. L., Kasinski, A. L., and Deng, Q. (2018) MicroRNA-223 Suppresses the
598   Canonical NF-kappaB Pathway in Basal Keratinocytes to Dampen Neutrophilic
599   Inflammation. *Cell Rep* **22**, 1810-1823
600 45. Truett, G. E., Heeger, P., Mynatt, R. L., Truett, A. A., Walker, J. A., and Warman, M. L.
601   (2000) Preparation of PCR-quality mouse genomic DNA with hot sodium hydroxide and
602   tris (HotSHOT). *Biotechniques* **29**, 52, 54
603 46. Kawakami, K., and Shima, A. (1999) Identification of the Tol2 transposase of the
604   medaka fish Oryzias latipes that catalyzes excision of a nonautonomous Tol2 element in
605   zebrafish Danio rerio. *Gene* **240**, 239-244